PERGAMON

Aerosol Science 33 (2002) 581–594

Journal of
Aerosol Science

www.elsevier.com/locate/jaerosci

Chemical classes of atmospheric aerosol particles at a rural site in Central Europe during winter

A. Held[a,*], K.-P. Hinz[b], A. Trimborn[b], B. Spengler[b], O. Klemm[a]

[a] *Bayreuth Institute for Terrestrial Ecosystem Research (BITÖK), University of Bayreuth, D-95440 Bayreuth, Germany*

[b] *Institute of Inorganic and Analytical Chemistry, Department of Analytical Chemistry, Justus Liebig University Giessen, D-35392 Giessen, Germany*

Received 26 July 2001; accepted 26 October 2001

Abstract

Ambient atmospheric particles were studied at an ecosystem research site in the Fichtelgebirge mountains in Central Europe by single-particle analysis and bulk impactor measurements. Fuzzy clustering analysis of mass spectra of individual aerosol particles allowed chemical classification of the atmospheric aerosol. During the campaign, inorganic salts, mineral particles, and carbonaceous particles, with varying degrees of secondary components, were identified. These chemical classes exhibited preferential size ranges leading to a characteristic pattern of relative abundances with respect to particle size. A more detailed analysis revealed that 65–80% of all particles were assigned almost exclusively to one chemical class. These particle populations are assumed to be externally mixed with respect to the identified chemical classes. The temporal variations of the ratio of nitrate to ammonium (ranging between 0.37 and 0.81) determined by both impactor measurements and single-particle analyses were in good agreement. Through Monte-Carlo-type simulations, confidence intervals of the mean NO_3^-/NH_4^+ ratio were calculated for sub-samples of the total particle population.

Keywords: Single-particle analysis; Fuzzy clustering; Internal/external mixing

1. Introduction

Aerosol particles play important roles in a variety of fields such as human health (Anderson, 2000) and technology (Deppert et al., 2000). Atmospheric aerosol particles also make essential

* Corresponding author. Tel.: +49-921-55-5622; fax: +49-921-55-5799.
E-mail address: andreas.held@bitoek.uni-bayreuth.de (A. Held).

0021-8502/02/$ - see front matter
PII: S0021-8502(01)00195-1

contributions to the atmosphere's chemical reactivity (Crutzen & Arnold, 1986; Dentener & Crutzen, 1993), influence the Earth's radiation budget both directly and indirectly (Charlson & Heintzenberg, 1995), and play a significant role in the deposition of atmospheric trace substances (Erisman et al., 1997).

Dry deposition of gases and particles affects the nutrient and pollutant budgets of ecosystems in a complex pattern. The quantification of dry deposition fluxes is a prerequisite for understanding changes in ecosystem behavior within a changing environment. However, the quantification of dry deposition fluxes onto terrestrial ecosystems is a challenging task, particularly over rough surfaces such as forest canopies (Foken, Dlugi, & Kramm, 1995; Peters & Eiden, 1992). Recently, vertical particle fluxes have been directly measured over forest canopies applying an eddy covariance system (Buzorius, Rannik, Mäkelä, Vesala, & Kulmala, 1998; Buzorius et al., 2000).

Combining vertical particle flux measurements and chemical composition data of aerosol particles may yield the input of constituents of particulate material through dry deposition. In order to improve these deposition estimates, two subjects may be considered. Firstly, for an accurate description of the physical properties of the atmospheric aerosol, size-resolved vertical particle flux measurements have to be developed. The mechanisms governing particle deposition vary considerably with particle size (e.g. Friedlander, 2000). Secondly, in order to take full advantage of size-resolved particle flux measurements, size-resolved chemical composition data is obligatory. However, as the atmospheric aerosol is a complex mixture of individual particles interacting with the surrounding gas phase in various ways, it is not sufficient to obtain size-resolved chemical composition data at bulk levels. Ultimately, the chemical composition of individual particles has to be determined because of the importance of particle interaction with their environment on the single-particle level (Hughes et al., 1999). Time-of-flight mass spectrometry is a powerful tool for online analysis of the chemical composition of individual aerosol particles (Suess & Prather, 1999; Johnston, 2000). Using individual particle analysis, it is possible to decide on the degree of internal/external mixing of the aerosol to assess the chemical variability of single airborne particles and thus their contribution to input of chemical species into ecosystems.

In this work, the classification results of single-particle mass spectra obtained during a field campaign in February 2000 are presented. The implications of these results for an assessment of internal or external mixing of ambient particle populations at a rural, forested site are discussed. Furthermore, the particle-to-particle variations of oxidized and reduced nitrogen are studied and these findings are compared to quantitative bulk measurements.

2. Site and methods

Ambient airborne particles were sampled at the ecosystem research site "Waldstein" of the Bayreuth Institute for Terrestrial Ecosystem Research (BITÖK) in Northern Bavaria, Germany, from February 1 to 18, 2000. This site is situated at 765 m a.s.l. at 50°09′N and 11°52′E, in the Fichtelgebirge, a mountain range near the German/Czech border. Measurements were conducted in a 100 m × 200 m forest clearing surrounded mainly by Norway Spruce (Picea abies (L.) Karst). Due to its geographical position in Central Europe, air masses of varying origin arrive at this site. Most of the time, especially in summer, westerly winds carrying marine air masses over Western and Central Europe to the site prevail. In wintertime, however, easterly winds advecting dry continental

air masses occur quite frequently. Long-term studies of air quality conditions have been successfully conducted since 1994 (Klemm & Lange, 1999).

We used the mobile time-of-flight mass spectrometer (TOF-MS) LAMPAS 2 for on-line analysis of the chemical composition of individual aerosol particles. A detailed description of this instrument can be found in Trimborn, Hinz, and Spengler (2000); only a brief explanation of the setup is given here. Ambient particles were introduced into the measuring system through a Rupprecht & Patashnick PM_{10} particle separator with an air flow of $16.7\,l\,min^{-1}$ (STP). A subsample of $1.6\,l\,min^{-1}$ was taken from a stainless steel tubing manifold of 1.2 m length with an isokinetical setup. The sample was introduced into the TOF-MS through a differentially pumped three-stage inlet module. The gas fraction of the air flow was pumped away yielding a particle beam that finally arrived at the ion source region of the mass spectrometer. Particles were detected by light scattering using a Nd:YVO4 laser ($\lambda = 532$ nm) as a light source. After particle detection, a delay generator was initiated to send a trigger signal to the pulsed ionization laser ($\lambda = 337$ nm) after a specified time. Particles were desorbed and ionized by laser desorption/ionization (LDI) and positive and negative mass spectra were obtained for each particle analyzed.

Sizes of particles to be analyzed were selected by setting appropriate delay times. In the inlet system, particles were accelerated until they had reached their terminal velocity, i.e. until they had obtained a characteristic velocity corresponding to their diameter (Dahneke, 1978). Because particles of different sizes have distinct terminal velocities, each individual particle travelled for a characteristic time between the plane of the detection laser and the plane of the ionization laser. By setting a constant delay time between particle detection and ionization, only particles of a defined size were hit for laser desorption/ionization.

Particles were analyzed in six different size classes, ranging from 0.2 to 1.5 μm aerodynamic particle diameter, for 10 min each hour. Using this configuration, all selected particle size classes were sampled within 1 h of measurement. The time resolution of LAMPAS 2 has been improved recently through implementation of an active triggering circuit for the ionization of each detected particle (Hinz, Trimborn, & Spengler, 2000).

It is too time consuming to obtain characteristic particle population patterns by inspecting each single-particle mass spectrum individually. Therefore, various statistical methods have been applied to classify single-particle spectra according to their chemical composition. These methods include Hierarchical Cluster Analysis (Xhoffer, Wouters, & Van Grieken, 1992; Treiger, Bondarenko, Van Malderen, & Van Grieken, 1995; Bondarenko, Treiger, Van Grieken, & Van Espen, 1996), Principal Components Analysis (Xhoffer et al., 1992; Hinz, Kaufmann, & Spengler, 1996), Neural Network Analysis (Ro & Linton, 1992; Song, Hopke, Fergenson, & Prather, 1999) and Fuzzy Cluster Analysis (Treiger et al., 1995; Bondarenko et al., 1996; Hinz, Greweling, Drews, & Spengler, 1999). The fuzzy clustering approach described by Hinz et al. (1999) based on the fuzzy-*c*-means algorithm (Bezdek, 1981) was used to classify our data. Mass spectra were grouped by particle size and day of analysis before the clustering procedure. No assumptions about the chemical composition of the aerosol particle population were made prior to classification. Between 150 and 250 particle spectra were typically used as the exclusive input data for a specific classification. "Mean" chemical classes were generated by the clustering algorithm itself. Thus, specific clustering results for different particle sizes and collection times were obtained.

For quantitative measurements, a five-stage Berner impactor with polyvinyl fluoride (Tedlar, DuPont) impaction surfaces was used as a reference sampler for concentration of ammonium,

nitrate and sulfate in aerosol particles ranging from 0.05 to 10 μm. The reduced pressure conditions of the Berner impactor may lead to evaporation of semi-volatile ammonium nitrate and ammonium chloride. However, we do not expect our measurements to be severely affected by the evaporation of ammonium nitrate. The sampling times were synchronized with single-particle analysis sampling intervals. Daytime measurements were run for 6 h, while overnight measurements were run for approximately 17 h. Ammonium ions were analyzed by flow injection analysis (FIA), nitrate and sulfate by ion chromatography (IC). Assuming both TOF-MS and impactor measurements to be representative for the ambient aerosol, qualitative and quantitative measurements were combined to yield semi-quantitative analysis of aerosol particles.

3. Results and discussion

3.1. Chemical classes of particles

During the field campaign more than 6000 bipolar mass spectra of single aerosol particles of different sizes on several days were obtained. Application of the fuzzy clustering analysis allowed clear identification of distinct chemical particle classes that could be visualized and interpreted analogously to measured single-particle spectra. These included inorganic salt particles, mineral particles and carbon particles containing varying degrees of secondary components and/or salts. In Fig. 1, a selection of five typical identified chemical classes is presented. The properties of these classes will be discussed in more detail below.

The spectra pattern in the top panel (Fig. 1a) is dominated by an ion signal indicating potassium K^+ ($m/z = 39$). Signals indicating sodium and iron can also be found in the positive ion pattern. In the negative ion pattern, signals of nitrate and sulfate are abundant. Therefore, particles of this type can be interpreted as inorganic salts.

Particles of the second class (Fig. 1b) always show clear signals of ammonium NH_4^+ ($m/z = 18$) in the positive ion spectrum and more pronounced signals of nitrate and sulfate than the first class. This indicates the presence of secondary components in these particles. Atmospheric trace gases such as NH_3, HNO_3 and H_2SO_4 most likely condensed and reacted onto already existing inorganic particles in the atmosphere before collection and analysis.

The third chemical class (Fig. 1c) represents particles with high signals at $m/z = 56$ (Fe^+) and $m/z = 48$ (Ti^+) indicating their mineral origin. Additional ion signals typical for mineral particles include Li^+ ($m/z = 7$), Al^+ ($m/z = 27$), TiO^+ ($m/z = 64$), FeO^+ ($m/z = 72$) and Fe_2O^+ ($m/z = 128$) as well as SiO_2^- ($m/z = 60$) and SiO_3^- ($m/z = 76$). The latter signals have been detected in a variety of single-particle spectra of mineral species, e.g. in quartz (Fletcher, 1989). Since the negative ion spectrum is dominated by nitrate and sulfate signals, and the positive ion spectrum contains ammonium ion signals, particles of this type contain secondary components as well.

The striking feature of the fourth class (Fig. 1d) is its pronounced pattern of carbon clusters at $m/z = 12, 24, 36, \ldots (C_n^+/C_n^-,\ n = 1 \cdots 10)$ in the positive and the negative ion pattern. Again, characteristic peaks of secondary components such as nitrate, sulfate and ammonium can be identified. These particles are classified as carbonaceous particles containing secondary components.

The last chemical class shown (Fig. 1e) can clearly be identified by the dominant carbon pattern and lack of significant signals of other ions. Since a characteristic peak pattern indicating organic

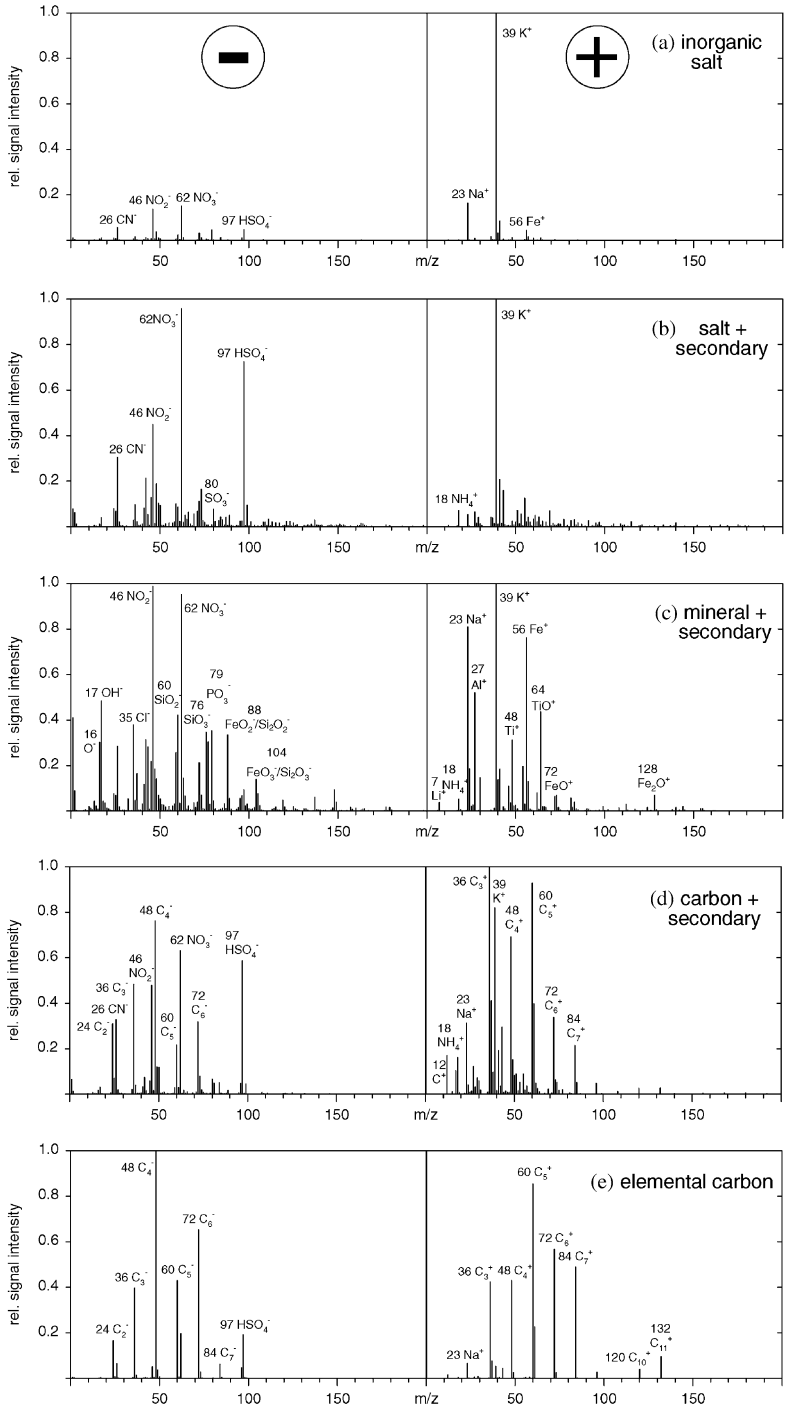

Fig. 1. Representative spectra patterns determined for particles evaluated in various size classes measured during the field campaign from February 1 to 18, 2000. Panels (a)–(d) from 1.0-μm-particles of February 6 (day), panel (e) from 0.5-μm-particles of February 7 (day).

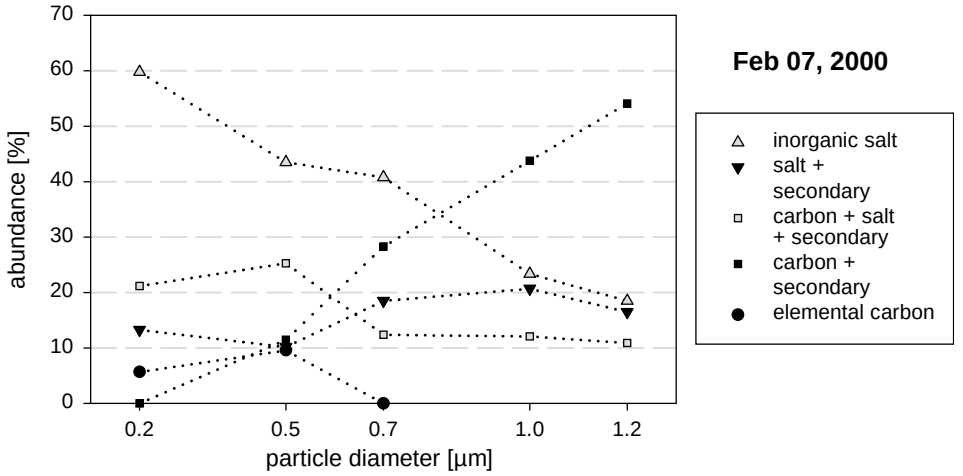

Fig. 2. Relative abundance of chemical classes vs. particle diameter for a particle population of February 7, 2000 (day). Class "carbon + salt + secondary" not shown in Fig. 1.

matter ($CHOO^-$ at $m/z = 45$, $C_2H_3O_2^-$ at $m/z = 59$, and $C_3H_5O_2^-$ at $m/z = 73$) was not found in the negative ion spectrum, these particles are assumed to consist of elemental carbon only.

Similar chemical classes have been found for different particle size ranges and on various days. This allows the direct comparison of class abundances depending on particle size, using a common set of basic particle classes. Weather conditions were essentially constant during the entire field campaign with westerly winds predominating, making it impossible to rigorously examine the dependence of chemical classification on varying atmospheric conditions. In the following section, a comparison of particle classes in different size classes is presented.

3.2. Size-segregation of chemical classes

It seems reasonable to expect certain chemical classes to occur more frequently in one particle size range than others. This is due to different particle formation mechanisms for accumulation mode and coarse mode particles. In Fig. 2, the relative abundance of five chemical classes is shown for different particle sizes on a single day of the campaign. These classes clearly exhibit preferential particle size ranges, which are discussed in detail below.

On February 7, five distinct chemical particle classes could be identified, including inorganic salt, salt with secondary components, carbon with salt and secondary components, carbon with secondary components and, finally, elemental carbon. The small size ranges were dominated by pure inorganic salt particles, whereas only a few particles containing secondary components were found. There is a sharp change in chemical composition at particle diameters of about 0.7 µm. No more elemental carbon particles can be found in larger particles while carbon with secondary components comprises more than 50% of the 1.2-µm-particles. Pure salt particles decrease rapidly down to 20% at 1.2 µm. The decrease of pure salt particles may be explained by secondary transformation processes occurring during atmospheric transport of the particle population. Atmospheric trace gases condense onto inorganic salt particles, causing them to grow. This results in a relative decrease of pure salt particles

with increasing particle size because there are only very few large salt particles without secondary components. At the same time, the relative abundance of carbon particles containing secondary components increases with increasing particle size due to condensation processes of atmospheric gases on carbon particles. Inorganic salt particles containing secondary components show their maximum relative abundance in the accumulation mode range from 0.7 to 1.0 μm. In this size range, most particle populations exhibit a maximum of total particle surface, which promotes condensation of gases onto preexisting particles. In particular, the uptake of NH_3 is expected in the accumulation mode, while HNO_3 uptake should be more important in larger particles (Fridlind & Jacobson, 2000; Fridlind et al., 2000).

Only a small number of elemental carbon particles can be found, exclusively in the two smallest size ranges. These pure carbon particles are assumed to be primary emissions from combustion or similar processes. As the measuring site is situated remotely from direct emission sources, the sampled particle populations have been exposed to various transformation processes during transport. Therefore, only very few pure carbon particles arrive at the site within the aged aerosol population. On several days, mineral particle classes could be identified. The relative abundance of these classes clearly increased with increasing particle size reflecting mechanical processes such as soil erosion that lead to mineral-containing particles within the coarse particle mode (e.g. Seinfeld & Pandis, 1998). Similar results were found for sodium-dominated classes (not shown in Fig. 1).

It must be concluded from this analysis that a joint chemical classification of the bulk population, including the entire size range, may lead to misinterpretation. If, for instance, the relative abundance of a specific chemical class is very small, this class may still be of importance in a certain particle size range.

3.3. Internal/external mixture

To illustrate the concept of the internal or external mixing state of the aerosol, we consider, for simplicity, particles of only one size class containing two chemical compounds, e.g., salt and carbon. If the salt is present exclusively in one group of the particles, and the carbon is exclusively present in the other group, the aerosol is externally mixed. The two chemical classes can be assigned to different origins, and exhibit different physical and chemical properties. Conversely, if each single particle contains an equal amount of salt and carbon, respectively, the entire aerosol is internally mixed (e.g., Friedlander, 2000; Seinfeld & Pandis, 1998). Intermediate states between these two extremes are most common in the atmosphere. For example, if three groups are present, one containing salt, the second one containing carbon, and the third one containing both chemical signatures, the aerosol is partly internally and partly externally mixed.

Fuzzy clustering is capable of assigning a single particle to more than one chemical class. Each single particle is assigned to all chemical classes through membership coefficients (MC) with values between 0 and 1. For each particle, the sum of all membership coefficients is one. If two or more MCs with similar values are assigned to a single particle, a high degree of diversity is indicated, while an MC value close to unity indicates good agreement between the single particle and the chemical class (Hinz et al., 1999).

In order to characterize the chemical composition of a given particle, it is often sufficient to evaluate the maximum membership coefficient, MC_{max}, which may assign this particle almost exclusively to one chemical class. Low MC_{max} values for single particles indicate a high degree

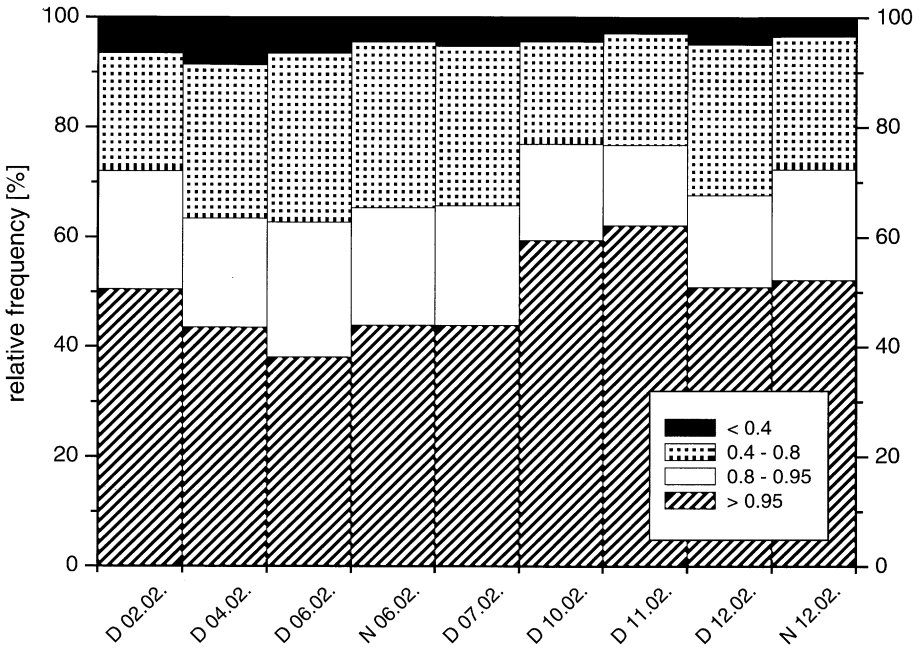

Fig. 3. Relative frequency of maximum membership coefficients > 0.95, between 0.8 and 0.95, between 0.4 and 0.8 and below 0.4. Particles with maximum membership coefficients under 0.4 are considered internally mixed. D: daytime measurements, N: nighttime measurements.

of internal mixing of an aerosol, while high MC_{max} values indicate a high degree of external mixing.

Confusion may occur because the definition of the chemical classes is in our case realized through a statistical process that does not respect the chemical identity of a salt or molecule. If a chemical class contains several chemical compounds, or if a chemical compound is assigned to several chemical classes, the MC_{max} values alone are not very good indicators of the degree of internal or external mixture of the aerosol. In other words, the better the chemical classification separates chemical compounds from each other, the better is the correlation between high MC_{max} values and the degree of external mixture of the aerosol. However, the definition of chemical classes through the statistical fuzzy analysis offers the unique opportunity to identify groups of particles with similar microphysical and chemical properties, irrespective of the specific sources of individual chemical compounds within these classes.

In Fig. 3, relative frequencies of the maximum membership coefficients are shown for all periods of measurement. During the entire field campaign, 65–80% of the particles are assigned predominantly to one chemical class ($MC_{max} > 0.8$). Applying an even stricter limit value of $MC = 0.95$, still 40–60% of all particles exhibit maximum membership coefficients greater than this value. In contrast, only 3–9% of the particles exhibit maximum membership coefficients below 0.4, i.e., they must be considered a mixture of different chemical classes. This means that in addition to a clear dependence of the chemical composition as a function of particle size (Fig. 2), particle populations are externally mixed within single size ranges with respect to the chemical classes identified.

Table 1
Single-particle statistics of five different populations: Number of evaluated particles, mean NO_3^-/NH_4^+ ratios and coefficients of variance of the five populations. Class II particles correspond to inorganic salt particles with secondary components (Fig. 1b)

	Total population			Only class II particles		
	Particle number	Arithmetic mean	CV (%)	Particle number	Arithmetic mean	CV (%)
February 6, day	313	0.83	97.6	109	0.73	67.8
February 6, night	611	0.47	97.5	241	0.51	75.5
February 7, day	463	0.34	103.1	120	0.40	90.2
February 12, day	126	0.54	87.2	57	0.63	81.4
February 12, night	340	0.64	90.1	133	0.80	81.7

3.4. Nitrate/ammonium ratio

Single-particle analysis can investigate chemical variability between individual aerosol particles. However, laser desorption ionization techniques allow at best semi-quantitative analysis of the concentration of individual particle components by using relative sensitivity factors (Mansoori, Johnston, & Wexler, 1994; Gross, Gaelli, Silva, & Prather, 2000). Despite this methodical limitation, a comparison of single-particle data and bulk impactor data was intended. An important issue regarding the atmospheric acid/base balance and the chemical composition of particulate matter relevant to ecosystems and plant nutrition is the concentration ratio of oxidized to reduced particulate nitrogen. The NO_3^-/NH_4^+ ratio of individual particles showed significant scatter due to analytical variability (LDI) as mentioned above, but also due to particle-to-particle variations in chemical composition.

The influence of external mixing of particles on the observed NO_3^-/NH_4^+ ratio was studied as follows. Firstly, individual NO_3^-/NH_4^+ peak area ratios were determined for a given population of particles. After that, NO_3^-/NH_4^+ peak area ratios were determined only for particles of a specific chemical class of this population. The coefficient of variance (CV) was used as a typical measure of the variability of the NO_3^-/NH_4^+ ratio in both cases. Table 1 lists coefficients of variance for a number of particle populations using the complete set of particles and also for a subset of the population, i.e. those from a specific chemical class.

In all cases, higher CV values for the total population as compared to the subset of particles of one specific chemical class were found. This indicates that there is a contribution to the ratio scatter resulting from variable particle composition, as mentioned above. It is also interesting to note that, except for one case (i.e. February 6, daytime), mean values of the NO_3^-/NH_4^+ ratio are always higher in the subsample than in the total population. This indicates that the chemical class of salt and secondary components (Fig. 1b) exhibits a slightly higher NO_3^-/NH_4^+ ratio than the entire particle population. Heterogeneous nucleation of NH_3 apparently played a larger role than that of HNO_3 in the atmospheric life of these particles. The exception on February 6 is probably due to the great dominance of mineral particles that was detected exclusively on this day. In our measurements, mineral particles always showed strong nitrate signals in the mass spectra, leading to an increase in the NO_3^-/NH_4^+ ratio of these particles.

Single-particle NO_3^-/NH_4^+ peak area ratios of a sampling period were averaged and corrected for instrument sensitivity by using a relative sensitivity factor (RSF). Since only little is known about

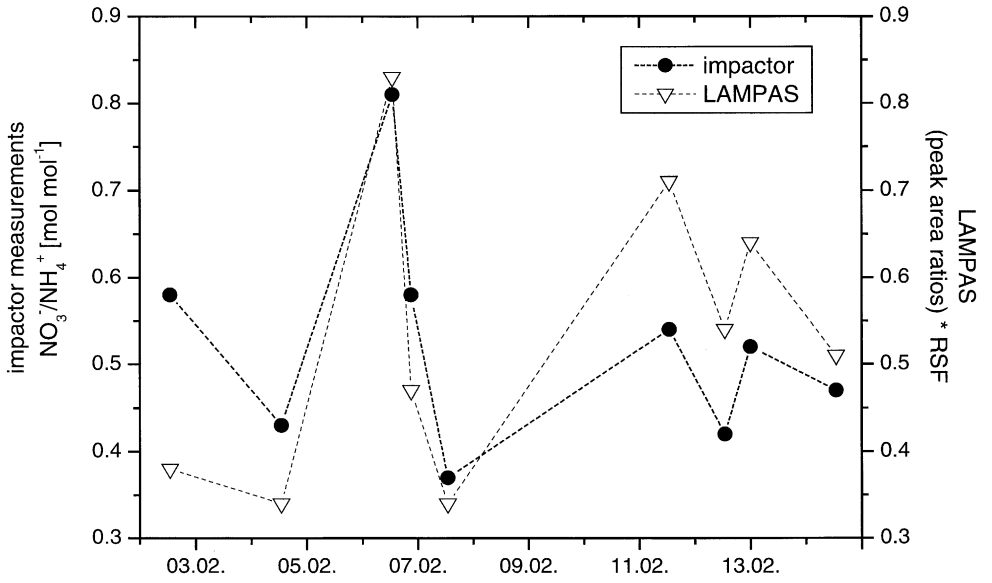

Fig. 4. Comparison of the particulate NO_3^-/NH_4^+ ratio determined by single-particle analysis vs. impactor measurements.

relative sensitivity factors, it was not possible to use RSFs determined independently. The RSF had to be obtained from our measurements through linear regression between the results of the impactor samples and the single-particle analysis data. This restricts our data interpretation to the analysis of temporal changes of the NO_3^-/NH_4^+ ratio (Fig. 4).

The temporal pattern of the LAMPAS data (triangles) matches the pattern of the impactor data (dots) very well. The NO_3^-/NH_4^+ ratio varied between 0.37 and 0.81 (impactor) and 0.34 and 0.83 (LAMPAS), respectively. These values indicate excess ammonium during the whole field campaign, which may be associated with anions other than nitrate, e.g. sulfate and chloride. Relatively high nitrate concentrations compared to ammonium on February 6 and 11 as detected with LAMPAS correspond to periods with a high share of mineral and sodium-containing particles. On these days, the aerosol composition is presumably governed by additional nitrate associated with sodium.

Single-particle spectra NO_3^-/NH_4^+ peak area ratios were averaged using a Monte-Carlo-type simulation routine in order to compare them to NO_3^-/NH_4^+ concentration ratios as determined by impactor measurements. From a given population, one particle ($i=1$) was chosen randomly, and if both ions were present, its ratio $(NO_3^-/NH_4^+)_{i=1}$ was determined. Then, a second particle ($i=2$) was randomly selected, combined with the first one, and the new ratio $(NO_3^-/NH_4^+)_{i=2}$ was calculated. This procedure was repeated until all particles of the sample had been combined (e.g., $i=1109$ on February 7). The entire calculation was repeated, starting with the random selection of a first particle, $k=10.000$ times. As a result, for any given sample size i, there is a population of k NO_3^-/NH_4^+ ratios, with a mean value and confidence interval.

Fig. 5 gives an impression of the changing distribution pattern as more and more particles (increasing i) are added to the subsample. The vertical axis represents the relative frequency of the k NO_3^-/NH_4^+ ratios for a given number of evaluated particles (i). The solid black lines indicate the

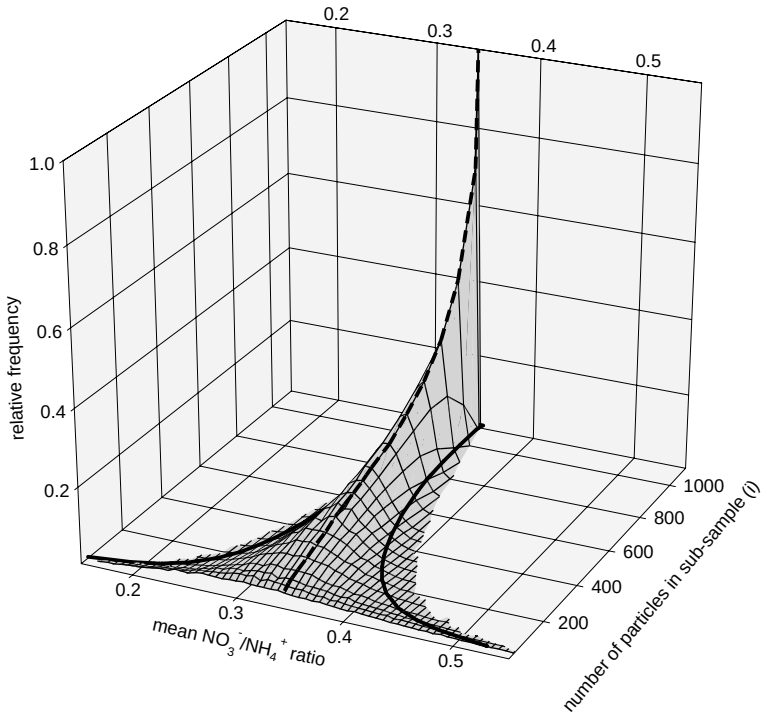

Fig. 5. Three-dimensional visualization of the frequency distribution of mean NO_3^-/NH_4^+ ratios vs. number of particles included in the subsample (Example shown for 07 February daytime data, $k = 10.000$ simulations).

95% confidence interval of the Gaussian distribution along the NO_3^-/NH_4^+ axis, whereas the dotted black line represents distribution modes. The confidence interval narrows as more particles are added to the subsample. When all particles are included, each simulation yields the mean NO_3^-/NH_4^+ ratio of the total population (i.e. 0.34 on February 7). It is interesting to note, however, that the distribution modes of all subsamples, i.e. even for small numbers of particles, are very close to this mean NO_3^-/NH_4^+ ratio of the total population, which is, according to Fig. 4, in good agreement with the quantitative impactor measurements. These results indicate that for the determination of a reasonable NO_3^-/NH_4^+ ratio (allowing 20% variation), about 200 particles need to be analyzed (95% confidence).

4. Conclusions

We were able to clearly identify distinct chemical classes of ambient aerosol particles using the LAMPAS TOF-MS system for data acquisition and fuzzy clustering for data analysis (Fig. 1). Each of these chemical classes could be interpreted in terms of possible particle formation and transformation processes. Between 65% and 80% of the analyzed particles exhibited a maximum membership coefficient of more than 0.8, i.e., most of the particle population was externally mixed with respect to the identified chemical classes. We found preferential particle size ranges for most chemical classes,

which is consistent with characteristic particle formation processes leading to variably sized particles. Trimborn, Hinz, & Spengler (2002) analyzed single atmospheric aerosol particles during the summer of 1998 at a site near Lindenberg (52°10′ N, 14°08′ E), about 275 km northeast of our site. They applied an identical analytical setup and data processing routine, and determined 10 chemical classes of atmospheric particles. Although they did not use any presumptions about possible chemical classifications as well, they arrived at a similar classification as presented above for the Waldstein site in winter.

The spectra patterns of inorganic salts, mineral/secondary particles, carbon/secondary particles and elemental carbon of both campaigns are in good agreement. However, chemical classes of sea salt particles could not be identified at the Waldstein site in contrast to the Lindenberg site, which is situated much closer to the sea. The persistance of aerosol particles free of secondary compounds at the rural Waldstein site seems to be correlated to certain atmospheric transport conditions. Analysis of the backward-trajectories revealed a relationship between the travel time of air masses over land (as compared to sea) and the relative content of secondary material. Fast and direct transport of air masses from the sea to our site yielded particle populations containing only a small fraction of secondary compounds.

Together with the fact that the aerosol population is mostly externally mixed, it is hypothesized from these observations that the identified chemical classes are typical components of the atmospheric aerosol in Central Europe. We suggest that it might be possible to identify a relatively small number of characteristic chemical classes sufficient to provide a framework for the description of aerosol particle populations on a regional scale.

There are at least two important implications of relatively low NO_3^-/NH_4^+ ratios in atmospheric aerosol particles: First, it indicates the degree to which the nitrogen gases NH_3 and HNO_3 contribute to the acidity of the particles. High contributions of nitrate (from condensation of gaseous HNO_3) lead to a high acidity, whereas NH_4^+ (from NH_3) would act as a buffer. The importance of these results must be evaluated together with the observed decrease of precipitation acidity (e.g. fog; Klemm, 2001) within the past two decades on a regional scale. Secondly, the ammonium ion is a nutrient for plants and microorganisms within the ecosystem that is generally more easily accessible than nitrate. Therefore, the deposition of particles with low NO_3^-/NH_4^+ ratios increases the nitrogen fertilization efficiency of atmospheric deposition for the forest ecosystems.

In conclusion, this study showed the potential gain in understanding of the atmospheric aerosol using single-particle analysis as compared to bulk methods. The atmospheric aerosol cannot be considered internally mixed, consisting of many identical particles. This variability has to be taken into account in modeling the particulate deposition into ecosystems, modeling heterogeneous processes modifying the atmospheric aerosol particle size distributions, and modeling the role of particles in the atmospheric radiation budget. However, our results also clearly exposed current limitations of available measuring systems for estimating particulate input of trace substances into ecosystems, which is still a highly complex task. The development of faster single-particle analysis systems could eventually lead to the possibility of direct measurements of vertical fluxes of particles and their constituents by use of eddy covariance techniques. This is probably one of the most promising approaches to link aerosol dynamics to quantitative ecosystem analysis for the next decade.

Acknowledgements

This work was funded by the Bundesministerium für Bildung und Forschung (BMBF) through Grant No. PT BEO 51-0339476 C. We appreciate the help and support of J. Gerchau, T. Wrzesinsky, and A. Mangold during the field experiment. Further, we are indebted to M. Schmidt for language-editing of the manuscript.

References

Anderson, H. R. (2000). Differential epidemiology of ambient aerosols. *Philosophical Transactions of the Royal Society of London*, *A 358*, 2771–2785.

Bezdek, J. C. (1981). *Pattern recognition with fuzzy objective function algorithms*. New York: Plenum Press, 256pp.

Bondarenko, I., Treiger, B., Van Grieken, R., & Van Espen, P. (1996). IDAS: A Windows-based software package for cluster analysis. *Spectrochimica Acta*, *B 51*, 441–456.

Buzorius, G., Rannik, Ü., Mäkelä, J. M., Vesala, T., & Kulmala, M. (1998). Vertical aerosol particle fluxes measured by eddy covariance technique using condensational particle counter. *Journal of Aerosol Science*, *29*, 157–171.

Buzorius, G., Rannik, Ü., Mäkelä, J. M., Keronen, P., Vesala, T., & Kulmala, M. (2000). Vertical aerosol fluxes measured by the eddy covariance method and deposition of nucleation mode particles above a Scots pine forest in southern Finland. *Journal of Geophysical Research*, *105*, 19 905–19 916.

Charlson, R. J., & Heintzenberg, J. (1995). *Aerosol forcing of climate*: *Report of the Dahlem workshop on aerosol forcing of climate*, Berlin 1994, April 24–29 (416pp.). New York: Wiley.

Crutzen, P. J., & Arnold, F. (1986). Nitric acid cloud formation in the cold Antarctic stratosphere: A major cause for the springtime 'ozone hole'. *Nature*, *324*, 651–655.

Dahneke, B. (1978). Aerosol beams. In D. T. Shaw (Ed.), *Recent developments in aerosol science*. New York: Wiley.

Dentener, F. J., & Crutzen, P. J. (1993). Reaction of N_2O_5 on tropospheric aerosols: Impact on the global distributions of NO_x, O_3, and OH. *Journal of Geophysical Research*, *98*, 7149–7163.

Deppert, K., Magnusson, M. H., Carlsson, S.-B., Gustafson, B., Junno, T., Montelius, L., Ohlsson, B. J., Samuelson, L., & Wernersson, L.-E. (2000). Future electronic devices by aerosol techniques. *Journal of Aerosol Science*, *31* (Suppl. 1), S532–S535.

Erisman, J. W., Draaijers, G., Duyzer, J., Hofschreuder, P., Van Leeuwen, N., Roemer, F., Ruijgrok, W., Wyers, P., & Gallagher, M. (1997). Particle deposition to forests — Summary of results and application. *Atmospheric Environment*, *31*, 321–332.

Foken, Th., Dlugi, R., & Kramm, G. (1995). On the determination of dry deposition and emission of gaseous compounds at the biosphere–atmosphere interface. *Zeitschrift für Meteorologie*, *4*, 91–118.

Fletcher, R. A. (1989). New way to mount particulate material for laser microprobe mass analysis. *Analytical Chemistry*, *61*, 914–917.

Fridlind, A. M., & Jacobson, M. Z. (2000). A study of gas–aerosol equilibrium and aerosol pH in the remote marine boundary layer during the first aerosol characterization experiment (ACE 1). *Journal of Geophysical Research*, *105*, 17 325–17 340.

Fridlind, A. M., Jacobson, M. Z., Kerminen, V.-M., Hillamo, R. E., Ricard, V., & Jaffrezo, J.-L. (2000). Analysis of gas–aerosol partitioning in the Arctic: Comparison of size-resolved equilibrium model results with field data. *Journal of Geophysical Research*, *105*, 19 891–19 903.

Friedlander, S. (2000). *Smoke*, *dust*, *and haze*: *Fundamentals of aerosol dynamics*. New York: Oxford University Press, 480pp.

Gross, D. S., Gaelli, M. E., Silva, P. J., & Prather, K. A. (2000). Relative sensitivity factors for alkali metal and ammonium cations in single-particle aerosol time-of-flight mass spectra. *Analytical Chemistry*, *72*, 416–422.

Hinz, K.-P., Kaufmann, R., & Spengler, B. (1996). Simultaneous detection of positive and negative ions from single airborne particles by real-time laser mass spectrometry. *Aerosol Science and Technology*, *24*, 233.

Hinz, K.-P., Greweling, M., Drews, F., & Spengler, B. (1999). Data processing in on-line laser mass spectrometry of inorganic, organic, or biological airborne particles. *Journal of the American Society for Mass Spectrometry*, *10*, 648–660.

Hinz, K.-P., Trimborn, A., & Spengler, B. (2000). Instrumental improvements in on-line laser mass spectrometry of aerosols. *Proceedings of the 48th ASMS Conference on Mass Spectrometry and Allied Topics*, Long Beach, 2000.

Hughes, L. S., Allen, J. O., Kleeman, M. J., Johnson, R. J., Cass, G. R., Gross, D. S., Gard, E. E., Gaelli, M. E., Morrical, B. D., Fergenson, D. P., Dienes, T., Noble, C. A., Liu, D.-Y., Silva, P. J., & Prather, K. A. (1999). Size and composition distribution of atmospheric particles in Southern California. *Environmental Science and Technology*, *33*, 3506–3515.

Johnston, M. V. (2000). Sampling and analysis of individual particles by aerosol mass spectrometry. *Journal of Mass Spectrometry*, *35*, 585–595.

Klemm, O. (2001). Trends in Fog Composition at a Site in NE Bavaria. *Proceedings of the second international conference on fog and fog collection*, 15–20 July 2001, St. John's, Newfoundland, Canada, 73–76.

Klemm, O., & Lange, H. (1999). Trends of air pollution in the Fichtelgebirge mountains, Bavaria. *Environmental Science and Pollution Research*, *6*, 193–199.

Mansoori, B. A., Johnston, M. V., & Wexler, A. S. (1994). Quantitation of ionic species in single microdroplets by on-line laser desorption/ionization. *Analytical Chemistry*, *66*, 3681–3687.

Peters, K., & Eiden, R. (1992). Modelling the dry deposition velocity of aerosol particles to a spruce forest. *Atmospheric Environment*, *26A*, 2555–2564.

Ro, C. U., & Linton, R. W. (1992). New directions in microprobe mass spectrometry: Molecular microanalysis using neural networks. *Microbeam Analysis*, *1*, 75–87.

Seinfeld, J. H., & Pandis, S. N. (1998). *Atmospheric chemistry and physics: From air pollution to climate change*. New York: Wiley, 1326pp.

Song, X.-H., Hopke, P. K., Fergenson, D. P., & Prather, K. A. (1999). Classification of single particles analyzed by ATOFMS using an artificial neural network, ART-2A. *Analytical Chemistry*, *71*, 860–865.

Suess, D. T., & Prather, K. A. (1999). Mass spectrometry of aerosols. *Chemical Reviews*, *99*, 3007–3035.

Treiger, B., Bondarenko, I., Van Malderen, H., & Van Grieken, R. (1995). Elucidating the composition of atmospheric aerosols through the combined hierarchical, non-hierarchical and fuzzy clustering of large electron probe microanalysis data sets. *Analytical Chimica Acta*, *317*, 33–51.

Trimborn, A., Hinz, K.-P., & Spengler, B. (2000). Online analysis of atmospheric particles with a transportable laser mass spectrometer. *Aerosol Science and Technology*, *33*, 191–201.

Trimborn, A., Hinz, K.-P., & Spengler, B. (2002). On-line analysis of atmospheric particles with a transportable laser mass spectrometer during LACE '98. *Journal of Geophysical Research*, in press.

Xhoffer, C., Wouters, L., & Van Grieken, R. (1992). Characterization of individual particles in the North Sea surface microlayer and underlying seawater: Comparison with atmospheric particles. *Environmental Science and Technology*, *26*, 2151–2162.